



## Thermodynamic Analysis of a Novel Air Preheating System

V.Beygzadeh<sup>a\*</sup>, Sh.Khalilarya<sup>b</sup>, I.Mirzaee<sup>b</sup>, V.Zare<sup>a</sup>, Gh.Miri<sup>c</sup>

<sup>a</sup>Faculty of Mechanical Engineering, Urmia University of Technology, Urmia, Iran \*Email: vbeygzadeh@gmail.com

<sup>b</sup>Mechanical Engineering Department, Faculty of Engineering, Urmia University, Urmia, Iran

<sup>c</sup>Department of Business Management, National Iranian Oil Refining & Distribution Company, Tehran, Iran

### ARTICLE INFO

Received: 08 Aug 2018  
Received in revised form:  
05 Dec 2018  
Accepted: 05 Dec 2018  
Available online: 15 Dec  
2018

### Keywords:

Thermodynamic  
analysis; solar air  
preheating system; air  
preheating;

### A B S T R A C T

A comprehensive thermodynamic analysis is used to characterize the exergy destruction rate in any part of the solar air preheating system (SAPHS) and calculate its efficiency. The system consists of a solar evaporator, a heat exchanger to air preheating and an auxiliary pump. A computer simulation program using EES software is developed to model and analyses the SAPHS. The system provides preheated air during the year.

The thermodynamic analyses involves the determination of effects of air preheating (APH) heat exchanger pinch point temperature, solar radiation intensity and overall heat loss coefficient of the solar evaporator on the performance of the SAPHS. The result showed that the main source of the exergy destruction is the solar evaporator. In the solar evaporator, 115.9 kW of the input exergy was annihilated. Other main source of exergy annihilation is the APHHE, at 7.45 kW. The overall energetic and exergetic efficiencies of the SAPHS were 70.11% and 9.766%, respectively.

© 2018 Published by University of Tehran Press. All rights reserved.

### 1. Introduction

Solar air heating is a renewable energy heating system used to heat or condition air for buildings or process heat [1]. A variety of systems can use SAH technologies to diminish the greenhouse gas emission from use of usual heat sources, such as fossil fuels, to make a sustainable way to generate thermal energy. SAH is a solar thermal system in which the energy from the sun, radiation, is captured by an absorbing system and used to SAPHS. The SAPHSs are economical, pollution free and easy for exploitation in countries like Iran (90% of the Iran country has enough sun to produce solar power 300 days a year. Iran has 0.520 kilowatts per hour per square meter of solar radiation every day. [2]). LHPs capacity may reach hundreds and thousands of watts [3]. A LHP, contains a heat pipe evaporator, a condenser, a liquid line, a vapour line and a compensation

chamber, is a two phase device that can carry heat all over a lengthy interval [4]. Huang et al. [5] Studied Low cost manufacturing of LHP for commercial applications. They conducted that during the last ten years, No any LHP failure was reported so far. Nishikawara and Nagano. [6] Accomplished optimization of evaporator wick shape in a LHP. They concluded that evaporator wick shape can be optimized by merely using the three phase contact line. Length. Jia et al. [7] Reviewed status and outlook of solar heat for industrial processes in China.

Hosseini et al. [8] thermodynamically modeled hybrid solar flameless combustion system. They showed that, the proposed system shows significant environmental benefits. Sharma et al. [9] Reviewed solar industrial process heating. Saxena et al. [10] reviewed SAHs and the different methods that are applied to better the thermal performance of SAHs.

The principal disadvantages of concentrated solar power technologies according to Pelay et al. [11] Review are as follows:

- PTCS: Relatively large space needed, low thermodynamic efficiency, low operating temperature.
  - LFRS: Low efficiency, low operating temperature.
  - SPTS: Large space needed, relatively high installation cost, high heat losses.
  - PDCS: Relatively high installation cost.
- But the LHPs have various benefits toward other systems [3]. The best applications for SAPHS are:
- Convenience with large open spaces such as factories.
  - Laboratories and agricultural facilities needing to continuously refresh air.
  - Facilities with a high daytime thermal load.
  - Thermal systems that can make a profit by taking preheated air (boilers, dryers, etc.).
  - Facilities that need low grade temperature heat.
- Because, cost effective SAPHS have many benefits, in this work, a new SAPHS with a SLHPE and an APH is thermodynamically analyzed. Executed works are as follows:
- Simulation and validation of the SAPHS.
  - Assess the efficacy of important designing

## 2. Materials and Methods

An APH is utilized to heat air before other process (for example, combustion in a mechanical system) with the principal purpose of enhancement the thermal efficiency of the process. In this sector, the specs of the SAPHS and its ingredients are expressed.

### 2.1. System description

Fig. 1 illustrates a SAPHS containing a SLHPE and an APHHE to produce preheated air.

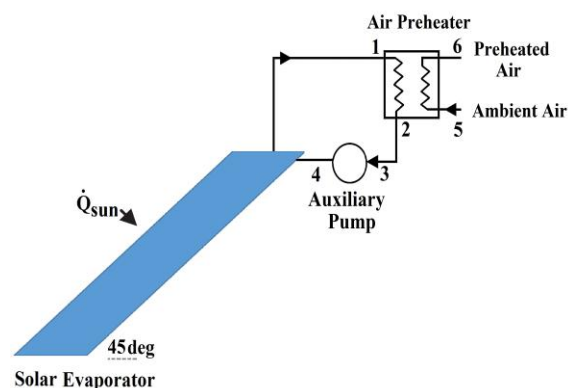


Figure 1. Schematic of the SAPHS

SAPHS is the transformation of sun energy into heat for APH using a SLHPE. The SLHPE heats a

working fluid (n-Heptane in this work, with the thermodynamic properties as shown in Table 1) that streams to the APHHE for air preheating and the SAPHS cycle is recurred continuously.

The schematic of the LHP and the LHP three direction evaporator are shown in Fig. 2.

To fulfill the thermodynamic analyses of the SAPHS, this presumptions are used:

- All the processes are at steady state.
- Thermal and radiation properties of the SLHPE are independent of temperature and heat losses from SAPHS are zero.
- The principle of ideal gas is used for the air.
- The SLHPS evaporators are not adiabatic and the flow regime in the SAPHS is laminar.
- Pressure drops in compensation chamber vapour and liquid lines, vapour and liquid headers are zero.
- The dead state is and .
- The surrounding temperature is .
- The mean solar radiation was 0.52 kW/m<sup>2</sup> (based on the mean annual solar radiation arriving to Iran).
- The APHHE pinch point temperature is 3 .
- Chemical exergy of system and the kinetic, potential energy and exergy are zero.

### 2.2. Thermodynamic modeling

In order to thermodynamic Simulation, the equations expanded are programmed using EES software. The input data used in this model are shown in Table 2.

To computer simulation the SAPHS, John A. Duffie et al. [13] procedure has been used. The computer simulation equations for the SAPHS are shown in Table 3. According to Chi SW. [12], the heat transportation limitation of the SAPHS is shown in Table 4.

## 3. Results & Discussion

In this sector, the results of analyses of the SAPHS are reported.

### 3.1. Validation of the SLHPE model

The SLHPE model is validated with the experimental study by E. Azad [14], as shown in Fig. 3. The model illustrates well agreement with the experimental work.

| Parameter                    | Value                          |
|------------------------------|--------------------------------|
| Chemical formula             | C <sub>7</sub> H <sub>16</sub> |
| Molar mass (kg/kmol)         | 100.21                         |
| Boiling temperature (°C)     | 98.42                          |
| Density (kg/m <sup>3</sup> ) | 684                            |
| Freezing temperature (°C)    | -90.549                        |
| Critical temperature (°C)    | 267                            |
| Critical pressure (MPa)      | 2.727                          |

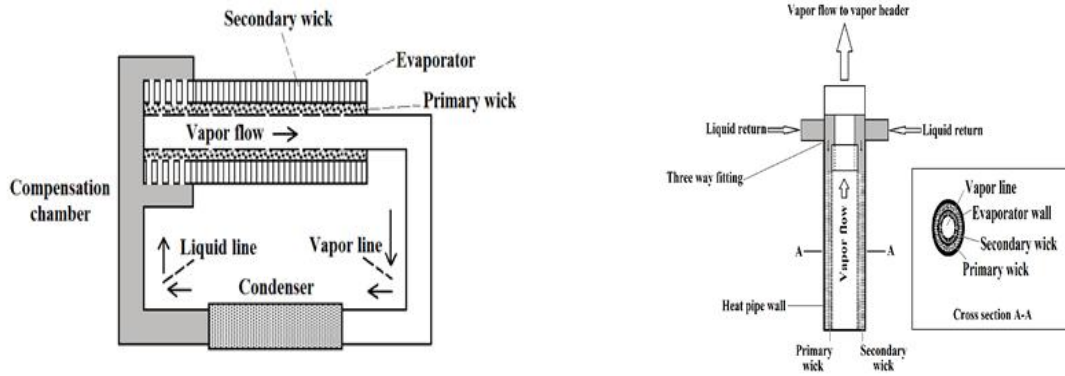


Figure 2. The schematic of the LHP and the LHP three direction evaporator

| Table 2. Input data for the SAPHS                                |                        |
|--|------------------------|
| SLHPE length, (m)  | 1.5                    |
| APH (SAPHS condenser) vapour pressure drop, (kPa)                | 5                      |
| Overall heat loss coefficient from SLHPE to ambient ( $kW/m^2$ ) | 0.005                  |
| Critical radius of boiling for toluene, (m)                      | 0.00000007             |
| SLHPE liquid pressure drop, (kPa)                                | 4                      |
| SAPHS operating temperature range                                | 100-125 <sup>0</sup> C |
| APHHE operating pressure range, (kPa)                            | 0-2500                 |
| Thickness of LHP wicks, (m)                                      | 0.0075                 |
| Thickness of LHP secondary wicks, (m)                            | 0.005                  |
| Thickness of LHP primary wicks, (m)                              | 0.0025                 |
| Liquid filling mass, (kg)  | 2.363                  |
| SLHPE slope  | 45°                    |
| LHPs type  | Mesh screen            |
| LHPs mesh ratio  | 2:1                    |
| APHHE height, (m)  | 2                      |
| number of LHPs   | 817                    |
| LHPs porosity  | 0.6363                 |
| Internal diameter of LHPs, (m)                                   | 0.049                  |
| Effective diameter of wick pores, (m)                            | 0.1111                 |
| APHHE conductivity, ( $W/m.K$ )                                  | 16                     |
| External diameter of LHP evaporators, (m)                        | 0.05                   |
| APH (SAPHS condenser) liquid pressure drop, (kPa)                | 1                      |
| Number of wick pores   | 9                      |
| LHP walls thickness, (m)   | 0.001                  |
| Thermal conductivity of evaporator walls, ( $W/m.K$ )            | 91                     |
| Thermal conductivity of evaporator wicks, ( $W/m.K$ )            | 91                     |
| SLHPE to APH height difference                                   | 1                      |
| Black nickel absorption factor ( $\alpha$ )                      | 0.96                   |
| Low content of Ferro oxide glass transmission factor, ( $\tau$ ) | 0.91                   |
| Gravity effect pressure, (kPa)                                   | +11.59                 |
| SLHPE vapour pressure drop, (kPa)                                | 7                      |
| SAPHS average stream speed, (m/s)                                | 50                     |

| Table 3. The computer simulation equations for the SAPHS  |   |
|---|---|
| $\dot{Q}_u = \dot{m}_1(h_1 - h_4)$  | The useful heat captured by the SLHPE   |
| $\dot{Q}_u = A_{SOL,EVA} F_R (S - U_l(T_4 - T_{amb}))$  | The useful energy produced by the SAPHS |
| $A_{SOL,EVA} = 0.75 \times N_{LHP} \pi D_o L_e$   | SLHPE area                              |
| $S = \eta_{LHP} G_b$  | radiation flux absorbed by the SLHPE    |
| $\eta_{LHP} = \tau \alpha$  | The LHP optical efficiency              |
| $\eta_{en,SOL,EVA} = \frac{\dot{Q}_u}{G_b A_{SOL,EVA}}$   | The energy efficiency of the SLHPE      |
| $\dot{E}_{SUN} = G_b A_{SOL,EVA} (1 + \frac{1}{3} (\frac{T_{amb}}{T_{SUN}})^4 - \frac{4}{3} (\frac{T_{amb}}{T_{SUN}}))$ | The exergy of the SLHPE                 |
| $T_{SUN} = 4500$  | Sun temperature                         |
| $\dot{I}_{SOL,EVA} = \dot{E}_4 - \dot{E}_1 + \dot{E}_{SUN}$   | exergy destruction of the SLHPE         |
| $\dot{m}_1(h_1 - h_2) = \dot{m}_5(h_6 - h_5)$   | APHHE energy balance                    |
| $\dot{I}_{APH} = \dot{E}_5 + \dot{E}_1 - \dot{E}_2 - \dot{E}_6$   | APHHE exergy balance                    |
| $\eta_{en} = \frac{\dot{Q}_{APH} - \dot{W}_{AUX}}{G_b A_{SOL,EVA}}$   | The energy efficiency of the SAPHS      |
| $\eta_{ex} = \frac{\dot{E}_6 - \dot{E}_5 - \dot{W}_{AUX}}{\dot{E}_{SUN}}$   | The exergy efficiency of the SAPHS      |

| Table 4. The heat transportation limitation of the SAPHS |         |
|--|---------|
| Operating limits   | Value   |
| Entrainment limit $\dot{Q}_{EL} (kW)$                    | 254.4   |
| Viscous limit $\dot{Q}_{VL} (kW)$                        | 10789   |
| Sonic limit $\dot{Q}_{SL} (kW)$                          | 42238   |
| Boiling limit $\dot{Q}_{BL} (kW)$                        | 74668   |
| Filled liquid Mass limit $\dot{Q}_{FL} (kW)$             | 219.434 |

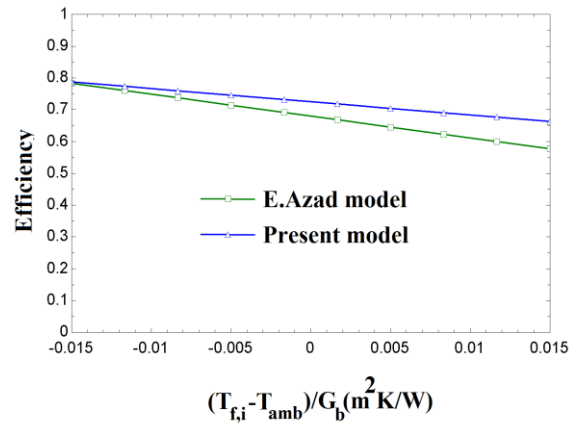


Figure 3. Validation of the SLHPE model as compared with E. Azad [14]

| Table 5. The thermodynamic properties of points for the SAPHS at demonstrated nodes in Fig. 1 |           |                  |        |         |           |             |                |
|---|-----------|------------------|--------|---------|-----------|-------------|----------------|
| State   | Fluid     | $\dot{m}$ (kg/s) | T (°C) | P (kPa) | h (kJ/kg) | S (kJ/kg.K) | $\dot{E}$ (kW) |
| 1   | N-Heptane | 0.2              | 120    | 183.7   | 532.7     | 1.437       | 20.84          |
| 2   | N-Heptane | 0.2              | 28     | 177.7   | 6.809     | 0.0223      | 0.02931        |
| 3   | N-Heptane | 0.2              | 28     | 189.3   | 6.819     | 0.0223      | 0.03272        |
| 4   | N-Heptane | 0.2              | 28     | 194.7   | 6.829     | 0.0223      | 0.03432        |
| 5   | Air       | 1.15             | 25     | 101     | 298.6     | 5.696       | 0              |
| 6   | Air       | 1.15             | 115.8  | 101     | 390       | 5.964       | 13.36          |

### 3.2. SAPHS energy and exergy analysis results

The thermodynamic properties of points for the SAPHS at demonstrated nodes in Fig. 1 are shown in Table 5.

The energy analysis results are shown in Table 6.

| Table 6. The results of energy analysis of the SAPHS |            |
|--|------------|
| SLHPE useful energy                                  | 105.2 kW   |
| APH energy flow                                      | 105.2 kW   |
| AUX pump input work rate                             | 0.00188 kW |
| SAPHS efficiency                                     | 70.11 %    |

The exergy analysis results are shown in Table 7, and show that the most exergy destruction occurs in the SLHPE (due to the major temperature difference in the SLHPE), which is 115.9 kW. As showed above, the major source of exergy destruction is the SLHPE and, thus, it can be used to find ways to diminish losses to make the SLHPE more efficient.

| Table 7. The results of exergy analysis of the SAPHS |              |
|--|--------------|
| SLHPE exergy destruction rate                        | 115.9 kW     |
| APH exergy destruction rate                          | 7.45 kW      |
| AUX pump exergy destruction rate                     | 0.0002792 kW |
| SAPHS efficiency                                     | 9.766 %      |

### 3.3. Effect of varying APHHE pinch point temperature on SAPHS performance

The APHHE pinch point temperature is an important design parameter in the SAPHS. Fig. 4 shows the change with APHHE pinch point temperature of the energy efficiency and exergy efficiency. As shown in this figure, increasing APHHE pinch point temperature increases the SLHPE, SAPHS cycle and APHHE exergy destruction rates. When the APH pinch point temperature increases, the heat captured by the APHHE diminishes, therefore the enthalpy of the preheated air in the APHHE diminishes, which diminishes the heat flow and increases the SLHPE, SAPHS cycle and APHHE exergy destruction rates and eventually leads to a diminution in the energy and exergy efficiencies of the SAPHS.

### 3.4. Effect of varying SRI on solar air preheating system performance

Another important parameter in the SAPHS is SRI because it affects the temperatures of the SAPHS. Fig.5 shows the variation of SAPHS energy and exergy efficiencies with SRI. As can be seen, increasing SRI, enhances the energy and

exergy efficiencies of the SAPHS, due to an increase in the SRI, diminishes the SAPHS cycle heat losses and exergy destruction rate.

### 3.5. Effect of varying overall heat loss coefficient of the SLHPE on SAPHS performance

The overall heat loss coefficient of the SLHPE ( $U_l$ ) is an important design parameter in the SAPHS. Fig. 6 shows the variation with ( $U_l$ ) of the energy efficiency and exergy efficiency. As shown in this figure, increasing ( $U_l$ ), diminishes the energy and exergy efficiencies of the SAPHS. When the ( $U_l$ ) increases, the heat captured by the SLHPE diminishes, therefore the enthalpy of the n-Heptane in the SLHPE diminishes, which diminishes the heat flow and eventually leads to a diminution in the energy and exergy efficiencies of the SAPHS.

## 4. Conclusions

In this work, the steady state thermodynamic analysis of the SAPHS is carried out. The major aim of this work is the modelling of a new SAPHS with SLHPE for use in industries (Petroleum refining, chemical processing, glass and metal industries, generation of steam and heating and drying of non-metal). The results of thermodynamic analysis showed that the main source of the exergy destruction is the SLHPE. In the SLHPE, 115.9 kW of the input exergy was annihilated. Other main source of exergy destruction is the APHHE, at 7.45 kW. The overall energetic and exergetic efficiencies of the SAPHS were 70.11% and 9.766%, respectively.

The major conclusions can be listed as follows:

- Increasing APHHE pinch point temperature increases the SLHPE, SAPHS cycle and APHHE exergy destruction rates.
- Increasing SRI, enhances the energy and exergy efficiencies of the SAPHS.
- Increasing overall heat loss coefficient of the SLHPE, diminishes the energy and exergy efficiencies of the SAPHS.
- SAPHS can diminish the fuel costs by means of extra heating energy through solar energy.
- SAPHSs reduce GHG emissions by diminish fossil based energies.
- The results of this research is useful to understand the performance of the SAPHSs.
- By preheating the air, damage to machinery can be prevented. Furthermore, it promotes higher savings in terms of energy by improving heating efficiency.
- By SAPHS, industrial systems that use high amounts of energy can experience considerable energy savings.
- It is expected SAPHS has the lowest cost and highest efficiency compared to other solar systems.

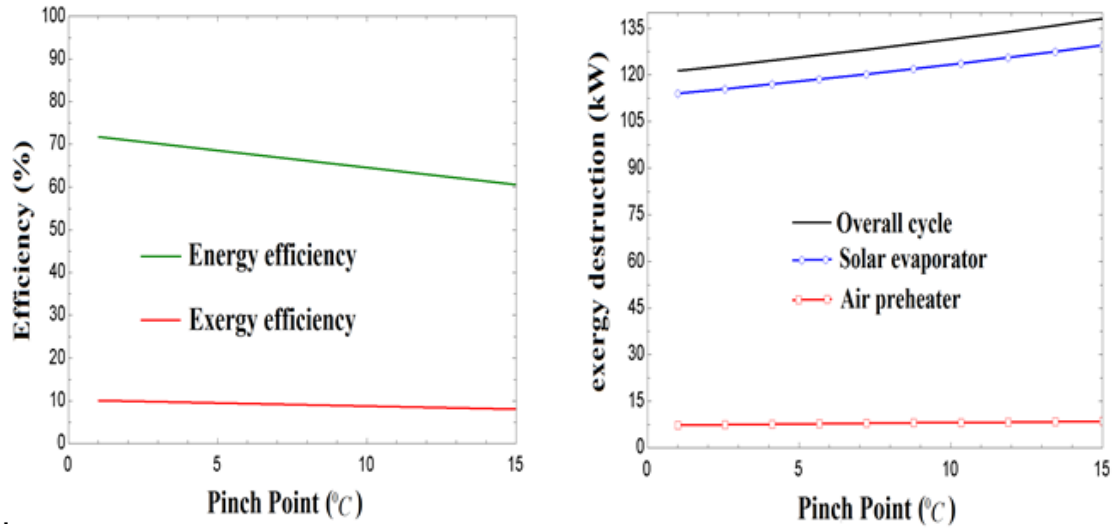


Figure 4. Change with APHHE pinch point temperature of the energy efficiency and exergy efficiency

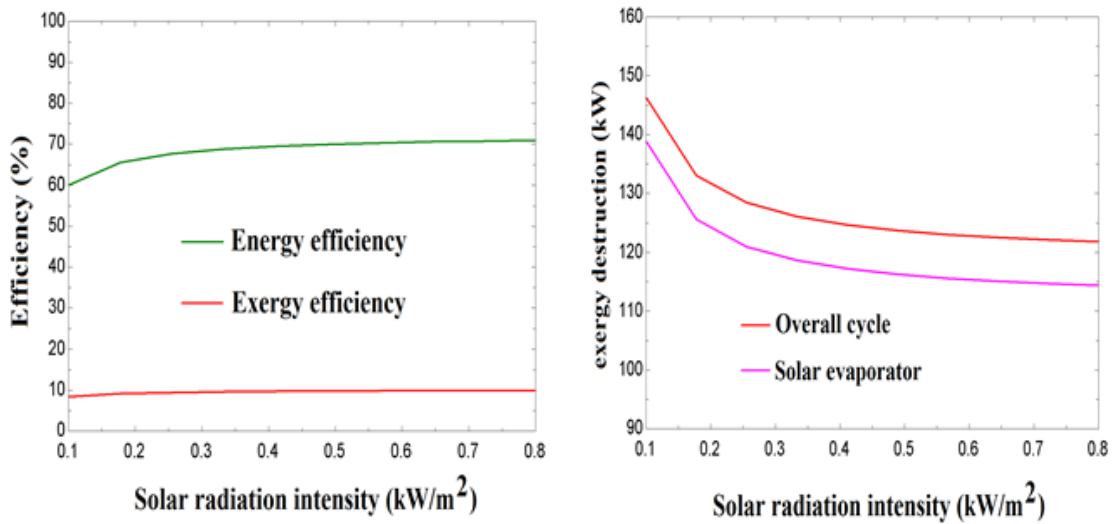


Figure 5. Change with solar radiation intensity of the energy efficiency and exergy efficiency

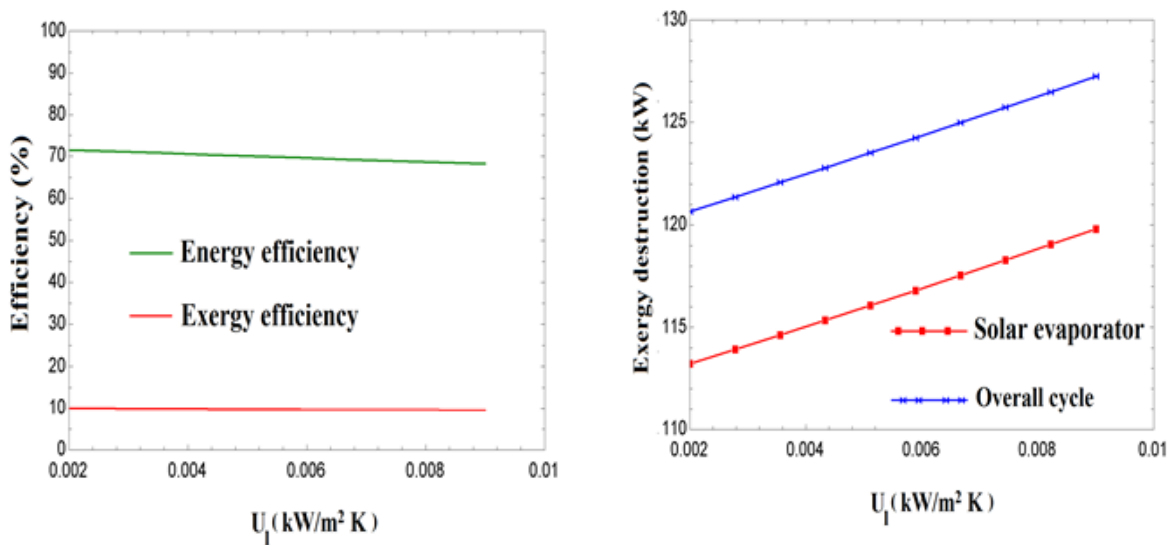


Figure 6. Change with overall heat loss coefficient of the SLHPE of the energy efficiency and exergy efficiency

## Acknowledgements

The author is grateful to the management and personnel of NIORDC for their technical support.

### i) Nomenclature

|                     |  |
|---------------------|--|
| APH                 | Air preheating or air preheater                            |
| APHHE               | air preheater heat exchanger                               |
| amb                 | ambient  |
| $A_{SOL,EVA}$       | The solar loop heat pipe evaporator area (m <sup>2</sup> ) |
| AUX                 | Auxiliary pump   |
| cv                  | control volume   |
| $\delta_{PW}$ (m)   | Thickness of LHPs primary wicks                            |
| $\delta_{SW}$ (m)   | Thickness of LHPs secondary wicks                          |
| $D_{ll}$            | Liquid line diameter                                       |
| $D_{vl}$            | Vapour line diameter                                       |
| $D_o$               | LHPs outer diameter  |
| $\delta_w$ (m)      | Thickness of LHPs wicks                                    |
| $\dot{E}_{heat}$    | Exergy transfer by heat, kW                                |
| $\dot{E}$           | Exergy rate, kW  |
| E                   | Energy   |
| e                   | exit   |
| F <sub>R</sub>      | LHP heat removal factor                                    |
| f, i                | fluid entering SLHPE                                       |
| G <sub>b</sub>      | solar radiation, kW/m <sup>2</sup>                         |
| h                   | specific enthalpy (kJ/kg)                                  |
| $\dot{I}$           | Exergy destruction rate (kW)                               |
| i                   | inlet  |
| LFRS                | Linear Fresnel reflector systems                           |
| $L_e$               | Solar evaporator length                                    |
| LHP                 | loop heat pipe   |
| $L_{ll}$            | Liquid line length   |
| $L_{vh}$            | Vapour header length                                       |
| $L_{vl}$            | Vapour line length   |
| $m_f$ (Kg)          | liquid filling mass  |
| $\dot{m}$           | Mass flow rate (kg/s)                                      |
| (Np)                | Number of wicks pores                                      |
| N <sub>LHP</sub>    | number of LHPs   |
| PTSC                | Parabolic trough collector systems                         |
| PDCS                | Parabolic dish collector systems                           |
| PWM                 | Number of meshes of primary wicks                          |
| P                   | pressure (kPa)   |
| $\dot{Q}_{FL}$ (kW) | Filled liquid Mass limit                                   |
| $\dot{Q}_{BL}$ (kW) | Boiling limit  |
| $\dot{Q}_{SL}$ (kW) | Sonic limit  |
| $\dot{Q}_{EL}$ (kW) | Entrainment limit  |

|                      |   |
|----------------------|---|
| $\dot{Q}_{VL}$ (kW)  | Viscous limit   |
| $\dot{Q}$            | Heat rate, kW   |
| SRI                  | solar radiation intensity                                       |
| SOL, EVA             | solar LHP evaporator  |
| SAH                  | solar air heating   |
| SLHPE                | solar loop heat pipe evaporator                                 |
| SPTS                 | Solar power tower systems                                       |
| SAHS                 | solar air heating system  |
| SAPHS                | solar air preheating system                                     |
| S                    | absorbed radiation by the SLHPE                                 |
| SUN                  | Sun   |
| s                    | specific entropy (kJ/kg-K)                                      |
| SWM                  | Number of meshes of secondary wicks                             |
| SAPHS                | solar air preheating system                                     |
| T                    | temperature °C or K   |
| T <sub>SUN</sub>     | Sun temperature (K)   |
| $U_l$                | Overall heat loss coefficient of the SLHPE, kW/m <sup>2</sup> K |
| u                    | useful  |
| $\dot{W}$            | Power or work rate, kW  |
| 0                    | reference environment condition                                 |
| <b>Greek symbols</b> |   |
| $\eta_{ex}$          | Exergy efficiency   |
| $\eta_{en}$          | Energy efficiency   |
| $\psi$               | Specific exergy, kJ/kg  |
| $\eta_{LHP}$         | LHP optical efficiency  |

## References

- [1] [https://en.wikipedia.org/wiki/Solar\\_air\\_heat#cite\\_note-14](https://en.wikipedia.org/wiki/Solar_air_heat#cite_note-14).
- [2] Iran Renewable Energy and Energy Efficiency Organization Annual report, 2010-2017.
- [3] Y. Maydanik, V. Pastukhov, M. Chernysheva. Development and investigation of a loop heat pipe with a high heat-transfer capacity. Applied Thermal Engineering (2018) 130: 1052–1061.
- [4] Min Yu, Thierno M.O. Diallo, Xudong Zhao, Jinzhi Zhou, Zhenyu Du, Jie Ji, Yuanda Cheng. Analytical study of impact of the wick's fractal parameters on the heat transfer capacity of a novel micro-channel loop heat pipe. Energy (2018) 158: 746-759.
- [5] Bin-Juine Huang, Yi-Hung Chuang, Po-En Yang. Low-cost manufacturing of loop heat pipe for commercial applications. Applied Thermal Engineering (2017) 126: 1091-1097.
- [6] M. Nishikawara, H. Nagano. Optimization of wick shape in a loop heat pipe for high heat transfer. International Journal of Heat and Mass Transfer (2017) 104: 1083–1089.
- [7] Teng jia, Junpeng Huang, Rui Li, Peng He, Yanjun Dai. Status and prospect of solar heat for

- industrial processes in China. *Renewable and Sustainable Energy Reviews* (2018) 90: 475–489.
- [8] Seyed Ehsan Hosseinia, Hasan Barzegaravval, Bruce Chehroudi, Mazlan Abdul Wahid. Hybrid solar flameless combustion system: Modeling and thermodynamic analysis. *Energy Conversion and Management* (2018) 166: 146–155.
- [9] Ashish K. Sharma, Chandan Sharma, Subhash C. Mullick, Tara C. Kandpal. Solar industrial process heating: A review. *Renewable and Sustainable Energy Reviews* (2017) 78: 124–137.
- [10] Abhishek Saxena, Varun, A.A.El-Sebaei. A thermodynamic review of solar air heaters. *Renewable and Sustainable Energy Reviews* (2015) 43: 863–890.
- [11] Ugo Pelay, Lingai Luo, Yilin Fan, Driss Stitou, Mark Rood. Thermal energy storage systems for concentrated solar power plants. *Renewable and Sustainable Energy Reviews* (2017) 79: 82–100.
- [12] Chi SW. *Heat Pipe Theory and Practice: A Source Book*, first edition. (1976), ISBN: 0070107181, Hemisphere Pub. Corp, 1976.
- [13] John A. Duffie, William A. Beckman. *Solar Engineering of Thermal Processes*, 4th Edition. (2013) pp.202-342, ISBN: 978-0-470-87366-3, New York: Wiley.
- [14] E. Azad. Assessment of three types of heat pipe solar collectors. *Renewable and Sustainable Energy Reviews* (2012) 16: 2833– 2838.